ISBN: 978-3-95450-241-7 ISSN: 2673-5350 doi:10.18429/JACoW-IBIC2022-TU1I2

DIAGNOSTICS WITH QUADRUPOLE PICK-UPS AT SIS18

Adrian Oeftiger*, Rahul Singh
GSI Helmholtzzentrum für Schwerionenforschung GmbH, Darmstadt, Germany

Abstract

The beam quadrupole moment of stored beams can be measured with a four-plate quadrupole pick-up. The frequency spectrum of the quadrupole moment contains not only the usual first-order dipole modes (the betatron tunes) but also the second-order coherent modes, comprising of (1.) (even) normal envelope modes, (2.) odd (skew) envelope modes and (3.) dispersion modes. As a novel diagnostic tool, the measured frequencies and amplitudes provide direct access to transverse space charge strength through the tune shift as well as linear coupling (and mismatch thereof), along with the benefit of a non-invasive beam-based measurement. Technically, quadrupole moment measurements require a pick-up with non-linear position sensitivity function. We discuss recent developments and depict measurements at the GSI SIS18 heavy-ion synchrotron.

INTRODUCTION

Quadrupolar pick-ups (QPU) in a beam line provide information about the coherent transverse second-order moments of a passing bunch of particles. These devices have often been used in studies measuring the beam emittance or injection mismatch of the optics functions [1–3], or the strength of space charge in synchrotrons [4–8]. The advantage is the non-invasive and thus non-destructive nature of measuring the quadrupolar moment S_{QPU} via induced currents in the four symmetrically arranged electrodes, in particular for inferring the transverse RMS emittances in comparison to destructive profile measurement methods like flying wire scans or secondary electron emission (SEM) grids. Typically, *time domain* oriented methods to determine the emittance from a measured quadrupolar moment demand well controlled experimental setups, where differential offsets in the quadrupolar moments need to be understood and controlled precisely while the strong dipole component in the signal needs to be suppressed. These challenges could possibly be the main reason why QPUs are typically not yet used as beam diagnostics in regular operation. A technically less demanding and thus potentially more rewarding approach in a synchrotron is to profit from the *frequency domain* and measure the bunch eigenmodes, where only the frequency content and not the absolute values of S_{QPU} matter.

The quadrupole spectrum of a circulating beam has a rich structure. Most often the two even transverse envelope modes of the oscillating $\sigma_{x,y}(s)$ are studied, most prominently for measuring the strength of space charge by determining the coherent tune shift of the envelope due to space charge defocusing. Past experiments mainly studied coasting beam conditions [4–7].

At the same time, space charge broadened resonances typically become an issue mostly under bunched beam conditions. A truly useful diagnostic tool for direct space charge strength quantification thus should be applicable to bunched beam. A recent study for the first time accomplishes this space charge measurement of bunched beams [8] at the CERN Proton Synchrotron (PS): since the envelope oscillations due to injection mismatch typically decohere very rapidly in bunches, they are much more challenging to measure than in coasting beams. As an alternative, the study establishes the quadrupole beam transfer function (Q-BTF) technique based on a transverse feedback system, which quadrupolarly excites the bunch in a frequency sweep while measuring the beam response in the QPU. Such measured "bands" of coherent envelope modes due to varying defocusing by space charge depending on the longitudinal line charge density are expected to reveal the maximum coherent envelope tune shift at the longitudinal peak line charge density.

Another notable finding from bunched beam Q-BTF measurements in Ref. [8] is the observation of the coherent dispersion mode. In Ref. [9] the connection of this mode to head-tail instabilities has been illuminated, as the dispersion mode locks onto the correlation between transverse displacement and longitudinal momentum. Furthermore, as also mentioned in Ref. [9], the space charge shift of the coherent dispersion mode frequency could in principle be used to quantify space charge as an alternative to envelope mode frequency shifts.

The quadrupole moment spectrum further contains the skew quadrupole resonances [9]. Their mode amplitude indicates injection mismatch with respect to linear coupling, which can be useful for a direct beam-based measurement. This approach again intrinsically includes space charge in contrast to conventional BPM-based methods such as the closest-tune approach $|C^-|$ [10], as dipole-moment-based measurements are insensitive to coupling contributions from space charge.

For bunched beam, the quantitative influence of chromatic detuning on the measured envelope bands has been raised as an open point, given its oscillatory nature due to synchrotron motion. Simulations in Ref. [8] demonstrate the significant widening of the measured envelope band width due to chromaticity. In this contribution we present new measurement results from the GSI SIS18 synchrotron, based on a recently established Q-BTF setup involving a quadrupole kicker and pick-up. While proton beams in CERN PS suffer from head-tail instabilities at intensities where space charge becomes relevant, (heavy-ion) beams in the SIS18 can reach significant space charge strength at lower intensities where head-tail instabilities play no significant role. SIS18 there-

* a.oeftiger@gsi.de

ISBN: 978-3-95450-241-7 ISSN: 2673-5350 doi:10.18429/JACoW-IBIC2022-TU1I2

fore provides stable measurement conditions when switching to zero chromaticity optics. We are hence in the position to compare the width of the envelope band measured both at natural and fully corrected chromaticity.

OVERVIEW

Four electrodes, symmetrically arranged in 90° steps in the transverse plane around the passing beam as indicated in Fig. 1, pick up on the quadrupolar moment of the passing beam by combining their induced voltages as $S_{\mathrm{QPU}} = (U_T + U_B) - (U_L + U_R)$ [11]. This quadratic signal

$$S_{\mathrm{QPU}} \propto \langle y^2 \rangle - \langle x^2 \rangle \tag{1}$$

contains contributions from all collective second-order modes coupling into the transverse plane, where x denotes the horizontal particle offset and y the vertical offset. The notation $\langle \cdot \rangle$ refers to the expectation value summing over all particles in the beam.

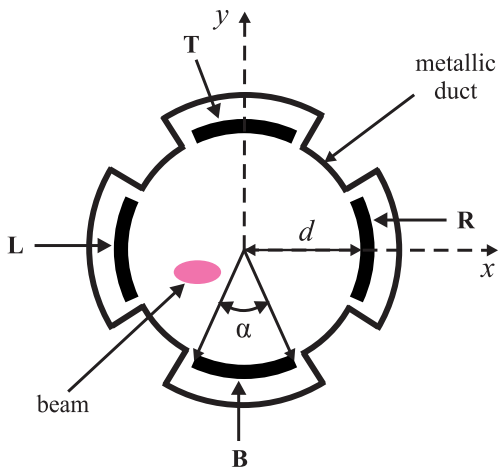

Figure 1: Schematics of four electrodes in quadrupolar pick-up, taken from Ref. [11].

Let us consider betatron motion x_β around a constant equilibrium orbit $\bar{x}$ with overlaid dispersive motion $D_x\delta$ for dimensionless momentum offset $\delta \doteq \frac{\Delta p}{p_0}$. D_x denotes the horizontal dispersion for this particle, $D_x = \partial x / \partial \delta$. The horizontal particle coordinate at the QPU location thus amounts to

$$x = \bar{x} + x_\beta + D_x\delta \,, \tag{2}$$

and likewise for the vertical plane. The collective quadratic signal thus splits up into

$$S_{\mathrm{QPU}} \propto \underbrace{\left(\langle y_\beta^2 \rangle - \langle x_\beta^2 \rangle\right)}_{\left(\sigma_y^2 - \sigma_x^2 + \langle y_\beta \rangle^2 - \langle x_\beta \rangle^2\right)} + 2 \cdot \bar{y} \, \langle y_\beta \rangle - 2 \cdot \bar{x} \, \langle x_\beta \rangle \tag{3}$$
$$+ \left\langle y_\beta \, \delta \right\rangle - \left\langle x_\beta \, \delta \right\rangle + \text{longitudinal } \delta \text{ terms} \,.$$

On top, for skew components in the focusing channel, additional coupling terms appear involving $\sigma_x\sigma_y$ and a skew envelope term σ_{xy}^2 (first discussed by Chernin [12]).

The spectral content of S_{QPU} comprises all the corresponding eigenmodes for these coherent first- and second-order moments. Given the bare betatron tunes $Q_{x,y}$, we thus conceptually expect to see

- $Q_{x,y}$: dipolar transverse motion from $\bar{x} \cdot \langle x \rangle$, $\bar{y} \cdot \langle y \rangle$,
- $2Q_{x,y}$: dipolar transverse motion from $\langle x_\beta \rangle^2$, $\langle y_\beta \rangle^2$,
- $2Q_{x,y} - \Delta Q_{x,y}^{\mathrm{env,SC}}$: horizontal and vertical even envelope modes from $\sigma_{x,y}^2$,
- $Q_{x,y} - \Delta Q_{x,y}^{\mathrm{disp,SC}}$: horizontal and vertical coherent dispersion mode from $\langle x_\beta \, \delta \rangle$, $\langle y_\beta \, \delta \rangle$, and
- $|Q_x - Q_y|, Q_x + Q_y$: odd envelope or Chernin modes from σ_{xy}^2, $\sigma_x\sigma_y$.

Note that this association of the two even envelope modes with a respective transverse degree of freedom is only valid for vanishing coupling. For full coupling, i.e. isotropic focusing $Q_x = Q_y$, the two modes become simultaneous anti-phase and in-phase oscillations of both planes, sometimes called "anti-symmetric" and "breathing" modes.

In general, the second-order modes are affected by coherent tune shifts due to direct space charge defocusing (unlike the first-order modes). This is indicated by $\Delta Q_{x,y}^{\mathrm{env,SC}}$ for the even envelope modes and by $\Delta Q_{x,y}^{\mathrm{disp,SC}}$ for the coherent dispersion mode (for further discussion see e.g. Ref. [13]).

The coherent tune shift of the odd envelope modes does not significantly depend on space charge under typical conditions of synchrotrons, as discussed by Aslaninejad and Hofmann [14], which is why we do not consider a corresponding ΔQ^{SC} term above. The odd envelope tunes coherently shift mainly due to the emittance ratio.

SIS18 SETUP

The GSI heavy-ion synchrotron SIS18 features two dedicated quadrupole electrode setups in section 4 (Fig. 2 in [7]) and section 12. Figure 2 displays the location of

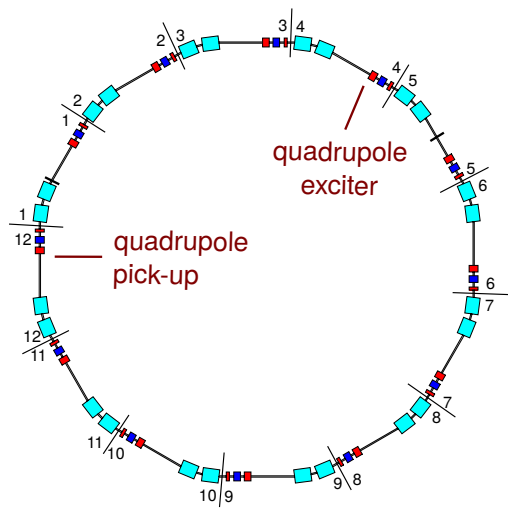

Figure 2: SIS18 survey with exciter and pick-up system to measure the quadrupole beam transfer function.

the quadrupole exciter and the pick-up in sectors 4 and 12,

ISBN: 978-3-95450-241-7 ISSN: 2673-5350 doi:10.18429/JACoW-IBIC2022-TU1I2

respectively. The β-function at the exciter location is exactly four times larger in the horizontal than in the vertical plane as can be seen in Fig. 3. Hence, the energy transfer to the beam is expected to be larger in the horizontal plane. These

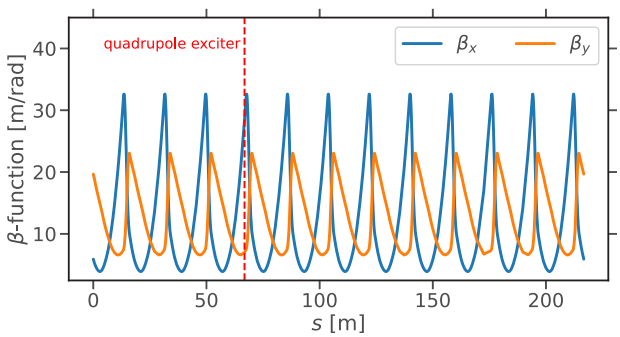

Figure 3: Twiss β-functions around SIS18.

two legacy capacitive pick-ups were utilized for quadrupolar excitation and the quadrupolar signal measurements, respectively. On the excitation side, the pick-up plates in section 4 were connected to a couple of 400 W 55 dB power amplifiers via magnetic-flux-based impedance transformers with a winding ratio of $\frac{n_2}{n_1} = 6$. The transformers are installed directly on the pick-up plates in the SIS18 tunnel and perform matching between the 50 Ω output impedance of the amplifiers to 100 pF capacitive load of the exciter plates. This quadrupole exciter system can provide a maximum power of 400 W which corresponds to a maximum voltage of 3 kVpp with a frequency range of 0.1 to 2 MHz. The frequency response of the excitation pathway is simulated via *spice* as shown in Fig. 4. For a maximum induced voltage of 2 kVpp,

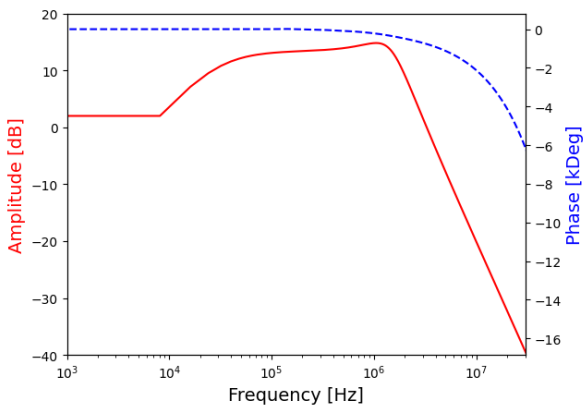

Figure 4: Simulated frequency response for the quadrupolar excitation path. 14 dB corresponds to factor 6 increase in the voltage applied on the plates with respect to the power amplifier output voltage. 3 dB reduction is seen at 100 kHz and 2 MHz defining the bandwidth of excitation system. The right axis depicts the phase response showing a large group delay introduced by the 80 m coaxial cable.

the simulated quadrupole field gradient in the exciter plates in shown in Fig. 5.

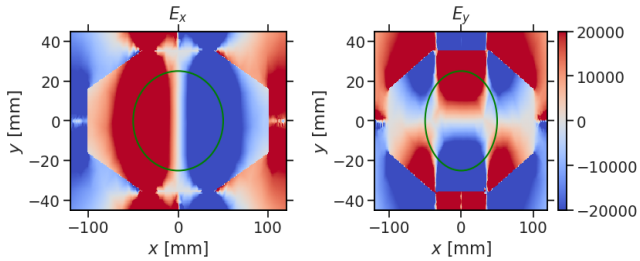

Figure 5: The static electric field components when 1 kV is applied on left and top plates while −1 kV is applied on right and bottom plates. E field units are in V/m.

The quadrupolar field gradient in the pick-up centre is $\approx 1.9\,\mathrm{MV/m^2}$ per plate which is used as input for the beam dynamics simulations. Other auxiliary components in the excitation set-up are a temperature monitor of the transformers and an attenuated signal from the plates for online monitoring.

On the acquisition side, the quadrupole pick-up in section 12 is utilised where each plate signal was digitised after 80 dB amplification by means of a 2 GHz, 250 MSa/s oscilloscope. The quadrupolar and dipolar signal reconstruction was carried out numerically followed by synchronization with the cavity rf signal. For comparison, the heaviest ions U^{238+} feature a revolution frequency of 150 kHz at injection energy.

The measurements have been conducted with lead ions Pb^{65+} at a low flat-top energy of 80 MeV/u equivalent to $B\rho = 4.2$ T m. The transverse geometrical rms emittances were evaluated via beam profiles measured with an ionisation profile monitor, determined as $\epsilon_x = 13$ mm mrad and $\epsilon_y = 11$ mm mrad at excitation start. The rf systems ran at a total of 6.3 kV and a harmonic of $h = 4$, the bunch length was estimated to a full width at half maximum value of 15.3 m. The bunch current amounted to 2 mA such that, at this energy, space-charge detuning becomes negligibly small with $\Delta Q^{KV} \lesssim 10^{-3}$. Doublet optics are employed with model tunes of $Q_x = 4.1$ and $Q_y = 3.22$. The envelope modes are thus expected around fractional tunes of $2q_x = 0.2$ and $2q_y = 0.44$, which sufficiently separates all modes simplifying the analysis of the measured spectra. The exciter rf signal has been swept between fractional tunes of 0.05 to 0.45 (about 25 to 250 kHz in baseband) to capture the beam response across the frequency range of interest. Q-BTF measurements have been recorded for both natural chromaticity ($Q'_x = -6.2$ and $Q'_y = -3.9$) and corrected chromaticity (using the two sextupole families with experimentally confirmed $|Q'_x|, |Q'_y| < 0.1$).

SIMULATION RESULTS

The experiment has been modelled in a particle tracking simulation with a detailed SIS18 lattice and including self-consistent space charge effects, based on the SixTrackLib [15] and PyHEADTAIL [16, 17] libraries. The results for a 10 ms duration of the sweep are shown in Fig. 6 for natural chromaticity and in Fig. 7 for corrected chromaticity.

ISBN: 978-3-95450-241-7 ISSN: 2673-5350 doi:10.18429/JACoW-IBIC2022-TU1I2

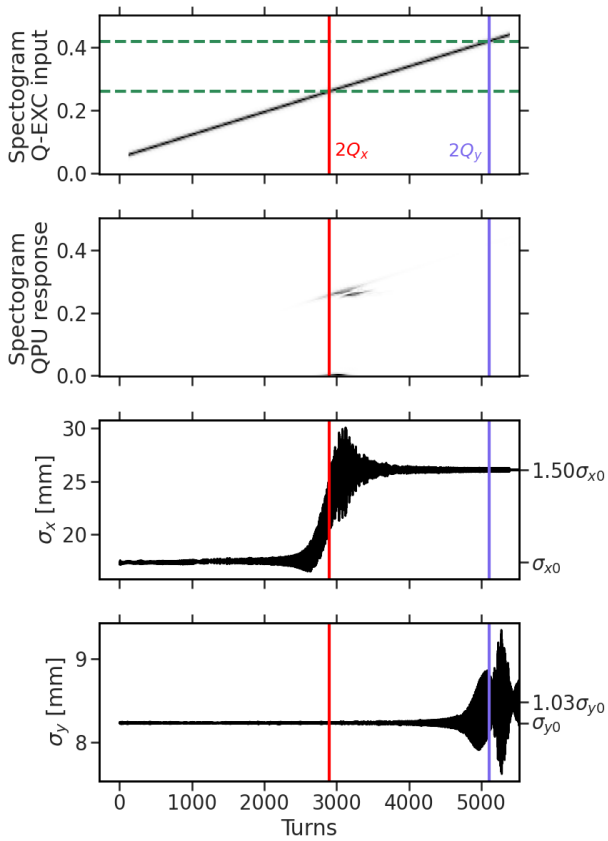

Figure 6: Q-BTF simulation at natural chromaticity.

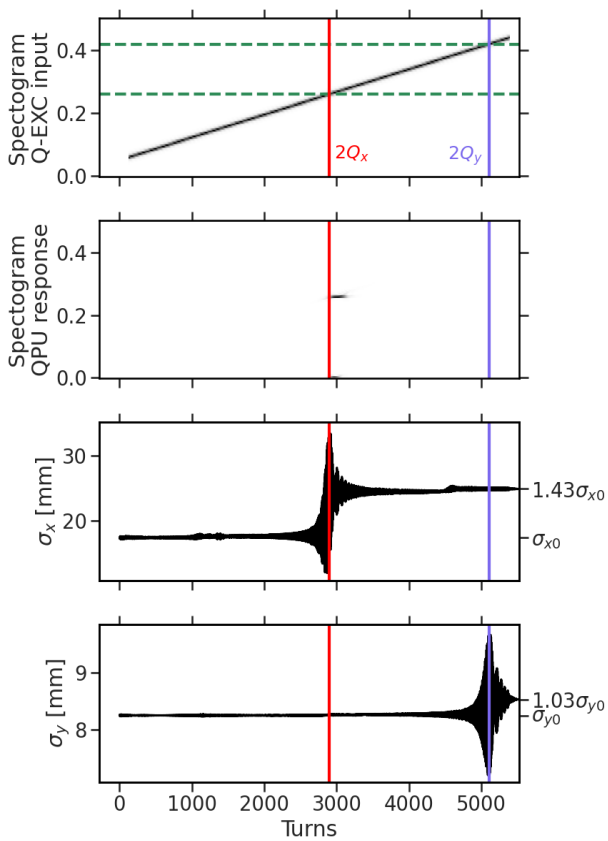

Figure 7: Q-BTF simulation at zero chromaticity.

The upper-most panel shows a spectrogram of the excitation signal, the second panel a spectrogram of the pick-up signal S_{QPU}, and the third and fourth panel the time evolution of the rms beam sizes in the horizontal and vertical plane, respectively.

The beam responds to the excitation signal with a clear oscillation in the horizontal and vertical beam sizes around the respective turns where the excitation frequency reaches $2q_x$ and $2q_y$. The average beam size increases indicating the emittance growth due to the envelope resonance. Irrespective of the chromaticity setting, the final beam size increased by about one and a half times in the horizontal and only marginally in the vertical plane. The QPU signal mainly exhibits the horizontal size oscillation in both displayed cases, the vertical oscillation is much smaller. The stronger effect in the horizontal plane originates in the larger horizontal β-function at the exciter.

A noticeable outcome of the simulations is the much narrower tune response in the corrected-chromaticity scenario. Figure 8 displays a comparison of the FFT-computed frequency spectra of S_{QPU}. The full width at half maximum of the horizontal envelope peak in the natural-chromaticity case is 2.3 times wider in comparison to the corrected-chromaticity case.

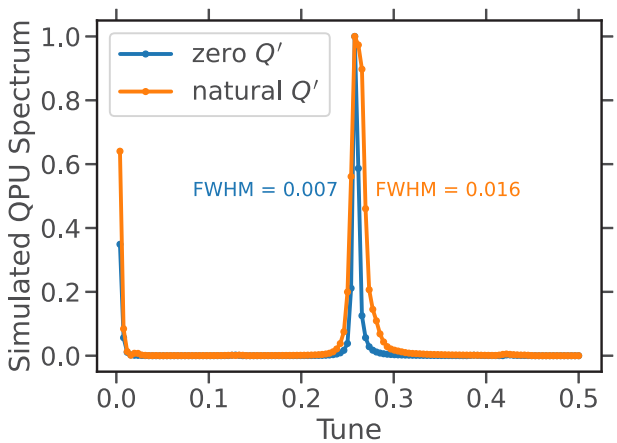

Figure 8: Comparison of simulated envelope resonances.

EXPERIMENTAL RESULTS

The turn-by-turn dipolar S_H, S_V and quadrupolar signals S_{QPU} were then reconstructed digitally using the relations, $S_H = (U_L - U_R)$, $S_V = (U_T - U_B)$ and $S_{\mathrm{QPU}} = (U_T + U_B) - (U_L + U_R)$. Simultaneously, beam current and transverse profiles were measured using a DC current transformer and ionisation profile monitors during the experiment. Figure 9 shows the quadrupolar spectrogram for natural chromaticity settings against a chirp excitation. The horizontal envelope mode excitation is more prominent in comparison to the vertical envelope mode in line with the simulations.

A comparison of the spectra for both chromaticities is shown in Fig. 10. The width of the envelope peak for corrected chromaticity is much narrower as predicted by simulations and points to a negligible chromatic tune spread.

ISBN: 978-3-95450-241-7 ISSN: 2673-5350 doi:10.18429/JACoW-IBIC2022-TU1I2

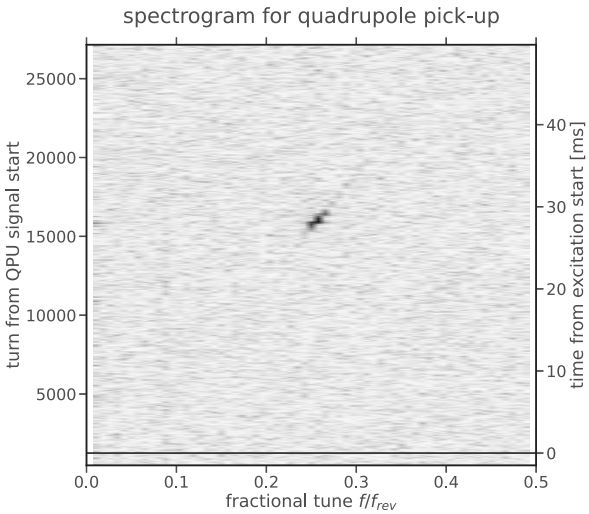

Figure 9: Quadrupolar spectrogram for natural chromaticity.

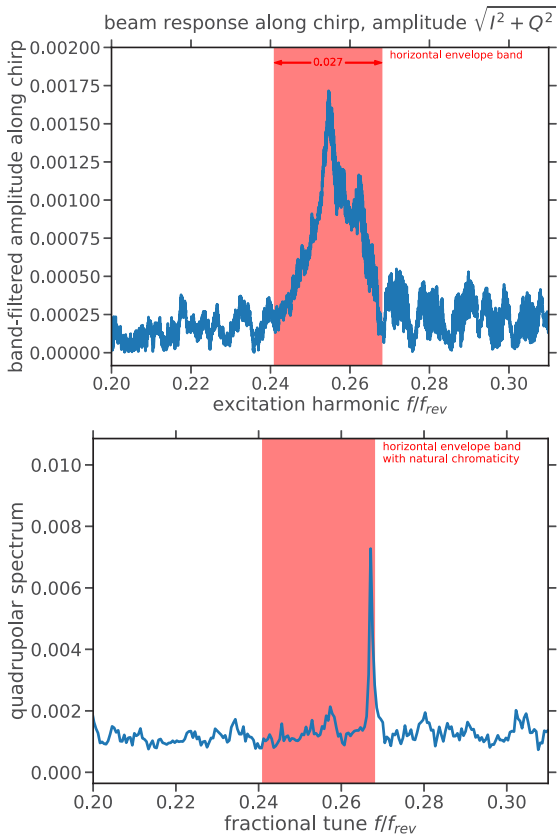

Figure 10: Quadrupolar spectra for natural chromaticity (top panel) and corrected chromaticity (bottom panel). The tune shift in the latter can be attributed to misaligned sextupoles.

The shift of mode frequency toward a larger value for corrected chromaticity can be attributed to uncorrected orbit in the sextupoles, which are powered to correct chromaticity. Figure 11 shows the sum signal of the quadrupolar pick-up.

A blow up in beam profile in both transverse planes as well as beam losses were distinctly observed at the horizontal and vertical envelope resonance excitation, respectively. The simultaneous measurement of the envelope mode frequencies and beam blow up clearly distinguishes between the excitation of second order dipolar modes and the envelope modes.

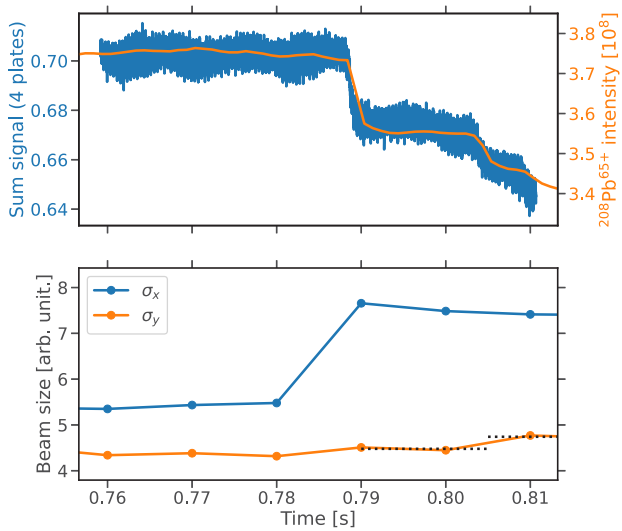

Figure 11: (Top) An overlay of the blue sum signal with the orange DCCT signal, (Bottom) Measured transverse profile widths as a function of time. The transverse blow up and losses coincide with the envelope mode excitation.

CONCLUSION

Following an overview of the expected modes in the quadrupole spectrum of a bunched beam, the quadrupole transfer function setup at GSI SIS18 has been discussed. First experimental results are well in agreement with the beam dynamics simulations of the experiment. The measurements demonstrate, for the first time, the considerable broadening of the envelope resonance width for bunched beams due to chromaticity.

ACKNOWLEDGEMENTS

The authors are grateful for the dedicated setup of the equipment by W. Kaufmann, for the support during the control room activities by O. Chorniy, B. Galnander, D. Rabusov, for technical support by S. Klaproth, C. Krüger, K. Lang, P. Niedermayer, T. Sieber, and to P. Forck and M. Schwickert for enabling this measurement campaign.

REFERENCES

[1] R. H. Miller, J. E. Clendenin, M. B. James, and J. C. Sheppard, "Nonintercepting emittance monitor", Stanford Linear Accelerator Center, Tech. Rep. SLAC-PUB-3186, 1983.

[2] A. Jansson, "Noninvasive single-bunch matching and emittance monitor", *Phys. Rev. ST Accel. Beams*, vol. 5, no. 7, p. 072 803, 2002. doi:10.1103/PhysRevSTAB.5.072803

[3] C.-Y. Tan, "Using the quadrupole moment frequency response of bunched beam to measure its transverse emittance", Fermi National Accelerator Laboratory (FNAL), Batavia, IL, Tech. Rep., 2007. doi:10.2172/919077

ISBN: 978-3-95450-241-7 ISSN: 2673-5350 doi:10.18429/JACoW-IBIC2022-TU1I2

[4] M. Chanel, "Study of Beam Envelope Oscillations by Measuring the Beam Transfer Function with Quadrupolar Pick-up and Kicker", in *Proc. EPAC'96*, Sitges, Spain, Jun. 1996, paper WEP014G, pp. 1015–1017. https://jacow.org/e96/PAPERS/WEPG/WEP014G.PDF

[5] T. Uesugi *et al.*, "Observation of Quadrupole Mode Frequency and its Connection with Beam Loss", in *Proc. PAC'99*, New York, NY, USA, Mar. 1999, paper TUP139, pp. 1821–1823. https://jacow.org/p99/papers/TUP139.pdf

[6] R. C. Bär, "Untersuchung der quadrupolaren BTF-Methode zur Diagnose intensiver Ionenstrahlen", Ph.D. dissertation, Universität Frankfurt, Germany, 2000.

[7] R. Singh *et al.*, "Observations of the Quadrupolar Oscillations at GSI SIS-18", in *Proc. IBIC'14*, Monterey, CA, USA, Sep. 2014, pp. 629–633. https://jacow.org/IBIC2014/papers/WEPD01.pdf

[8] A. Oeftiger, "Requirements and Results for Quadrupole Mode Measurements", in *Proc. HB'18*, Daejeon, Korea, Jun. 2018, pp. 393–398. doi:10.18429/JACoW-HB2018-THA1WE02

[9] A. Oeftiger, "Diagnostics with quadrupolar pick-ups", in *CERN Yellow Rep. Conf. Proc.*, Zermatt, Switzerland, Sep. 2019, vol. 9, pp. 130–136. doi:10.23732/CYRCP-2020-009.130

[10] G. Guignard, "The general theory of all sum and difference resonances in a three-dimensional magnetic field in a synchrotron; part 1", CERN, Tech. Rep., 1975. https://cds.cern.ch/record/323328

[11] J. A. Tsemo Kamga, W. F. O. Müller, and T. Weiland, "Analytical and numerical calculation of the second-order moment of the beam using a capacitive pickup", *Phys. Rev. Accel. Beams*, vol. 19, no. 4, p. 042 801, 2016. doi:10.1103/PhysRevAccelBeams.19.042801

[12] D. Chernin, "Evolution of RMS beam envelopes in transport systems with linear X-Y coupling", *Part. Accel.*, vol. 24, pp. 29–44, 1988. http://cds.cern.ch/record/1053510

[13] Y. S. Yuan, O. Boine-Frankenheim, G. Franchetti, and I. Hofmann, "Dispersion-induced beam instability in circular accelerators", *Phys. Rev. Lett.*, vol. 118, p. 154 801, 15 2017. doi:10.1103/PhysRevLett.118.154801

[14] M. Aslaninejad and I. Hofmann, "Effect of space charge on linear coupling and gradient errors in high-intensity rings", *Phys. Rev. ST Accel. Beams*, vol. 6, p. 124 202, 2003. doi:10.1103/PhysRevSTAB.6.124202

[15] M. Schwinzerl, H. Bartosik, R. D. Maria, G. Iadarola, A. Oeftiger, and K. Paraschou, "Optimising and Extending a Single-Particle Tracking Library for High Parallel Performance", in *Proc. IPAC'21*, Campinas, Brazil, May 2021, pp. 4146–4149. doi:10.18429/JACoW-IPAC2021-THPAB190

[16] A. Oeftiger, "An Overview of PyHEADTAIL", CERN, Tech. Rep. CERN-ACC-NOTE-2019-0013, 2019. https://cds.cern.ch/record/2672381

[17] A. Oeftiger and S. Hegglin, "Space Charge Modules for PyHEADTAIL", in *Proc. HB'16*, Malmö, Sweden, Jul. 2016, pp. 124–129. doi:10.18429/JACoW-HB2016-MOPR025